J. exp. Biol. **126**, 157–179 (1986)
Printed in Great Britain © *The Company of Biologists Limited 1986*

PHASE-DEPENDENT MODULATION OF AUXILIARY SWIMMERET MUSCLE ACTIVITY IN THE EQUILIBRIUM REACTIONS OF THE NORWAY LOBSTER, *NEPHROPS NORVEGICUS* L.

BY DOUGLAS M. NEIL AND JALEEL A. MIYAN*†
Department of Zoology, University of Glasgow, Glasgow G12 8QQ, Scotland

Accepted 16 July 1986

SUMMARY

1. The activity of swimmeret muscles of the lobster *Nephrops norvegicus* during beating in the upright and tilted animal has been examined. The responses to tilt are produced primarily by stimulation of the statocysts.

2. The anatomy of the swimmeret muscles is described. Although essentially similar to previous descriptions, important new aspects are presented.

3. The arrangement of the main powerstroke and returnstroke muscle groups in relation to the peg-and-hook articulation of the swimmeret produces a segregation of action, with different muscles contributing progressively to force production.

4. The auxiliary muscles of the basipodite, M9, M10 and M13 act to twist the swimmeret laterally. The auxiliary muscle M11–12–14–15 acts to maintain a rearward powerstroke.

5. The innervation of swimmeret muscles and the location of their motoneurone cell bodies in the abdominal ganglia have been revealed by cobalt staining. There is a clear segregation of powerstroke and returnstroke motoneurones. Intraganglionic fibre tracts as well as four interganglionic fibres are identified.

6. Intracellular studies on the twister muscles show that M9 receives at least three excitatory units, and M10 at least six. No inhibitory activity was ever recorded in these muscles. M9 and the medial bundle of M10 receive tonic excitatory inputs, while the lateral bundle of M10 receives phasic inputs and is normally silent in the absence of lateral beating.

7. In the absence of swimmeret beating, body roll about the long axis induces tonic motor activation of the lateral twister muscles (M9 and M10) and the returnstroke muscles in the swimmerets on the side tilted upwards.

8. When beating occurs it is predominantly in the swimmerets tilted upwards, and there is an entrainment of phasic activity in M9, M10 and M13 to the powerstroke phase of the beats. Tonic units to the returnstroke muscle remain unaffected.

9. The results are discussed with particular reference to the interaction of descending statocyst information with the central pattern generator for swimmeret beating.

* Present address: Department of Zoology, University of Edinburgh, West Mains Road, Edinburgh EH9 3JT, Scotland.
† To whom reprint requests should be addressed.

Key words: Crustacea, lobster, swimmeret, equilibrium.

INTRODUCTION

Stereotyped equilibrium reactions in decapod crustaceans have proved most suitable systems in which to determine the input–output characteristics of motor reflexes (Neil, 1985). Much attention has been paid to the postural reactions of cephalic, thoracic and abdominal appendages, which show tonic or phasic responses to static tilts (Hisada & Neil, 1985). However, equilibrium imbalance is generated in many cases as a consequence of an animal's own locomotory behaviour, and it is therefore of great relevance to examine the interaction between the motor systems producing locomotory propulsion and the sensory systems detecting equilibrium.

In propulsive movements such as the rapid tail flexion of macrurous decapods, steering and righting can be accomplished by alterations in the line of action of the propulsive system, which is the whole abdomen in this case (Reichert & Wine, 1983; Newland, 1985). In addition, asymmetrical changes in the attitude of particular appendages, primarily the uropods, cause turning and righting torques to be generated by the tail flexion (Newland, 1985). Movements of the latter type are specifically associated with the powerstroke, i.e. flexion, the appendages being 'feathered' on extension to reduce opposing drag forces. The action of this auxiliary steering system is therefore incorporated at only one particular phase of the propulsive cycle.

Coordination of this type must be even more extensive in rhythmic locomotory systems such as those for walking and swimming in crustaceans, and flying in insects. In these cases a non-phased sensory input from exteroceptors must interact with the rhythmical activity of one or more central pattern generators, to modify their output without disrupting the underlying propulsive pattern. It is more straightforward to examine such interactions in locomotion through a uniform medium such as air or water, rather than in limb-based terrestrial locomotion in which the additional requirement for support is also involved. Much recent interest has been shown in these aspects of steering control by exteroceptive cues in the locust flight system (Reichert, Rowell & Griss, 1985). In the Crustacea, the swimmerets of lobsters and crayfish provide a suitable system for such a study, since they display a closely coupled metachronal beating (Hughes & Wiersma, 1960) and respond with clear righting reactions to disruptions in equilibrium (Davis, 1968*a*). This paper reports our examination of the neuromuscular basis of swimmeret beating in the Norway lobster, *Nephrops norvegicus*, with particular reference to the control of lateral beating as an example of a righting reaction.

MATERIALS AND METHODS

Male and female specimens of the Norway lobster, *Nephrops norvegicus*, from the Firth of Clyde were supplied by the Universities Marine Biological Station, Millport, Isle of Cumbrae. After removal of their chelipeds by autotomy, they were kept in an aerated aquarium supplied with circulating sea water, and fed on heart meat once per week. Animals measuring between 10 and 25 cm from rostrum to telson were used in the experiments.

The anatomy of the swimmerets was studied in living or freshly killed animals. The innervation was stained with reduced Methylene Blue (Pantin, 1946), by injection into the base of the swimmeret approximately 30 min prior to dissection. Nerves stained deep blue, with little staining of muscle fibres. The innervation and central neuroanatomy was also stained by filling axons with cobalt through their cut ends (Sandeman & Okajima, 1973; Altman & Tyrer, 1980). Nerves were filled *in vivo* through their cut ends immersed in a droplet of 200 mmol l^{-1} cobalt chloride solution in distilled water, within a Vaseline bath. After 12–24 h the swimmeret and associated ventral nerve cord were removed, washed in sea water and, if necessary, further dissected. Cobalt sulphide was precipitated with a concentrated solution of ammonium sulphide in sea water (for up to 90 min). The preparation was fixed in a solution of 10 % formalin in sea water, dehydrated in an ethanol series, and cleared in methyl salicylate. The cobalt/nickel differential staining method of Quick & Brace (1979) was also employed to demonstrate the central and peripheral terminations of different nerve branches. Selected branches were filled with 200 mmol l^{-1} nickel chloride solution, or a 200 mmol l^{-1} solution of cobalt chloride and nickel chloride in equal proportions. After incubation, precipitates of different colours were obtained by immersion in saline containing a few drops of saturated rubeanic acid (dithiooxamide: Sigma Chemicals Ltd) in absolute alcohol. Some of these fills were also intensified by the method of Bacon & Altman (1977).

Material for histological sectioning was fixed with 4 % glutaraldehyde in phosphate-buffered saline, post-fixed with 1 % osmium tetroxide, dehydrated in ethanol and embedded in Araldite resin. Sections were cut at 1 μm and stained with Methylene Blue for light microscopy. Thin sections were mounted on grids and stained with uranyl acetate and lead citrate for transmission electron microscopy.

The neurophysiological experiments were performed with the animal mounted in an apparatus for administering tilt stimuli about the longitudinal axis. For myographic, suction and hook electrode recordings, the whole animal was secured, ventral side up, on a cradle mounted on horizontal bearings. Sinusoidal oscillations of up to $\pm 45°$ were produced by a variable-speed motor connected *via* an eccentric arm and drive bar to one end of the cradle. Electrodes were held in micromanipulators (Prior type MM2) mounted on stereotactic arms of the cradle. For intracellular recordings, the anterior portion of the animal was detached from the cephalothorax and secured in a small cradle, mounted on a horizontal bearing. This allowed the 'head' to be tilted without disturbing the abdomen, which was secured on a bed of wax (Miyan, 1984). The whole preparation was immersed in oxygenated saline.

Myographic recordings were made using 100 μm diameter plastic-coated copper wire, or 76 μm diameter Teflon-coated silver wire. Two twisted lengths were inserted together through the cuticle into a particular muscle bundle. Nerve recordings were made using suction or hook electrodes. Gold-plated suction electrodes of plastic or glass were made according to the design of Theophilidis & Burns (1982), and the hook-in-oil design was adapted from that of Wilkens & Wolfe (1974). Signals from these electrodes were fed through an Isleworth A101 differential preamplifier and

recorded on a Racal Thermionic FM tape recorder. Records were either filmed from the face of an oscilloscope using single-shot and moving-film photography, or analysed using computer-assisted techniques (Neil, Barnes & Burns, 1982).

RESULTS

The sensory basis of the equilibrium response

The detection of body tilt and the subsequent reflex drive of equilibrium reactions are performed by a number of sensory systems (Neil, 1982, 1985; Hisada & Neil, 1985), and to establish which of these is involved in the control of the swimmeret tilt response a number of control experiments were performed. Davis (1968*a*) found the statocyst organs to be of primary importance in *Homarus* and, in confirmation of this, we found that removal of the statoliths from both organs (without disruption of the chambers themselves) completely eliminated the swimmeret response to tilt in *Nephrops*. This finding also suggests that the lith hair system, which is sensitive to linear accelerations of the overlying lith, is primarily involved. The free thread hairs, which monitor angular accelerations through the inertial properties of the fluid in the statocyst chamber (Neil & Wotherspoon, 1982), were not disturbed in the operation, and presumably therefore have little influence on the swimmeret response.

Another sensory input recently shown to have a powerful influence over righting responses arises from the stimulation of leg proprioceptors by relative movements between the animal and the substrate on which it is standing (Schöne, Neil, Stein & Carlstead, 1976). Such an effect may well occur onto lobster swimmerets (Miyan, 1982; Neil, 1985), but its contribution was excluded in our experiments by performing the tilts in mid-water.

The contribution of vision to the compensatory eye reactions of decapod crustaceans is extremely strong (Neil, 1982), but its influence on righting reactions of the thoracic and abdominal appendages is always weak, or totally absent (Neil, 1985). The swimmeret response of *Nephrops* is undiminished if performed with a well-illuminated stationary visual surround, although this may be as much a result of the breakdown of visual pigment in animals kept in normal daylight (Loew, 1976; Shelton, Gaten & Chapman, 1985) as of a lack of a reflex connection from eyes to swimmerets. All experiments described here were performed under normal room illumination.

Other general influences on the swimmeret tilt response arise from the abdominal posture assumed by the animal. When the abdomen was held in a flexed posture the swimmerets showed no overt response to body tilt. However, when the tail was extended there was clear tilt-related behaviour. Such an interaction between the motor activity in the abdominal axial musculature, and the expression of equilibrium reflexes in abdominal appendages has also been described by Takahata, Yoshino & Hisada (1981) for crayfish uropods. The results of tilt experiments described below were obtained from animals which were actively extending their abdomens.

Anatomy of the swimmeret muscles

The major anatomical features of the swimmeret musculature of *Nephrops norvegicus* follow the description given by Davis (1968*b*) for the lobster *Homarus americanus*, and therefore only new aspects of functional significance will be presented here. The nomenclature and numbering also follow Davis (1968*b*).

The swimmerets are located in sockets on the ventral abdominal sternal ribs. A hook formed from the medial coxopodite articulates with a curved peg arising from the ventral abdominal rib in such a way that the swimmeret is free both to move in an anterior–posterior plane, and to rotate about its own axis (Fig. 1A). Apart from this single articulation, the joint is surrounded by thick articular membrane.

From their origins on the lateral abdominal wall, the main powerstroke (PS) muscle bundles project to their insertions on sclerites in the posterior articulation membrane (Fig. 1B). The PS muscles are arranged in two groups (M4–6 and M7–8) with separate origins but insertions on adjacent sclerites. The various returnstroke (RS) muscles share a common origin on the lateral abdominal wall. Their bundles then diverge, so that M3 inserts on a sclerite in the anterior articulation membrane, while M1–2 enters the swimmeret basipodite, forming a tendon (tendon C of Davis, 1968*b*) which passes around the articular peg and inserts on the posterior surface of the medial coxopodite (Fig. 2). M17–18 also runs to this tendon from the medial basipodite wall.

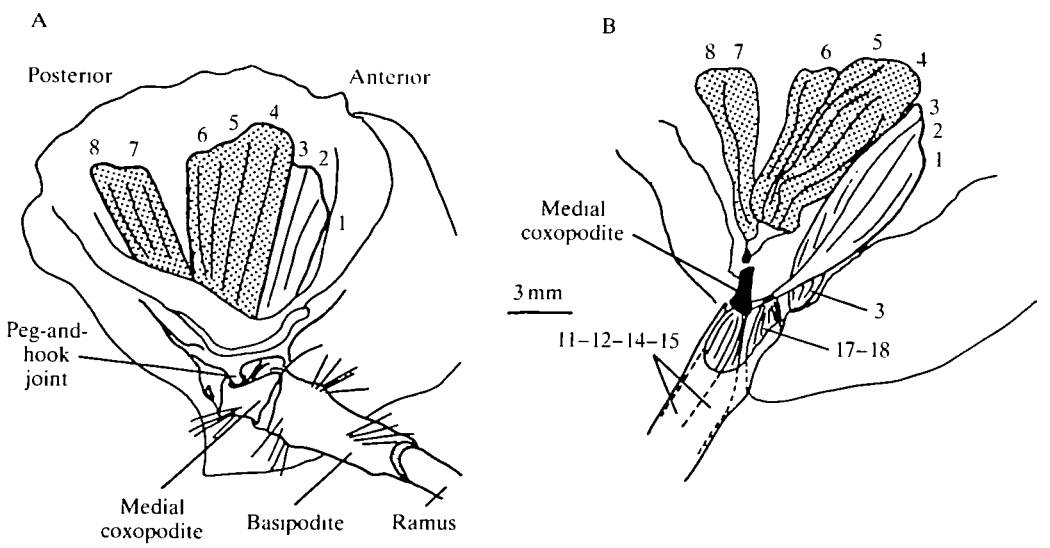

Fig. 1. (A) Left ($N = 3$) swimmeret of *Nephrops norvegicus* viewed from a medial aspect to show the peg-and-hook joint of the medial coxopodite with the sternal rib, the basipodite and the rami. The origins of the main returnstroke (RS) muscles (M1–3) and the main powerstroke (PS) muscles (M4–8) (stippled) on the lateral abdominal wall are indicated. (B) Same view with articulation removed to show the insertions of the main PS muscles (stippled) and RS muscles, and the relationship between the RS muscle bundles M1–2 and M17–18.

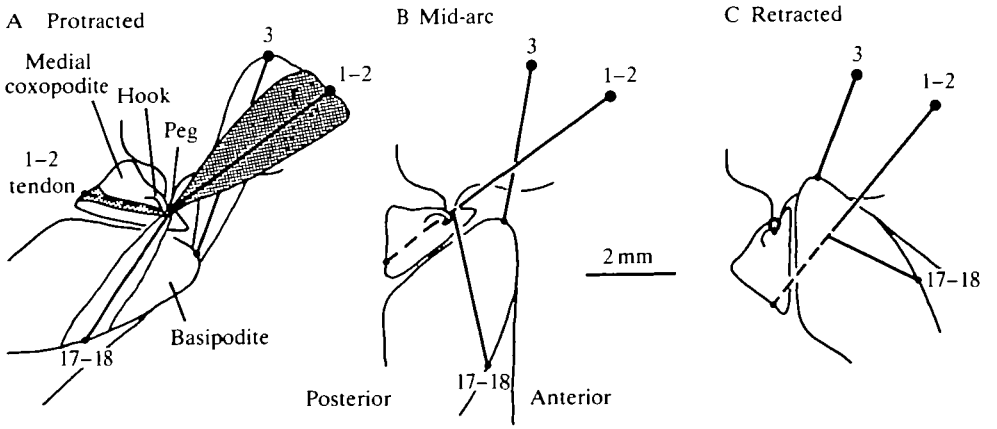

Fig. 2. Diagrams of the positions of the returnstroke (RS) muscles M1–2 and M17–18 in relation to the peg-and-hook of the joint in the right swimmeret, at three points in the swimmeret movement arc, viewed from a lateral aspect. Muscle outlines are shown only in A. M1–2 muscle and tendon are shown stippled. Lines of action of the muscles are indicated by solid lines (and dashed lines for the M1–2 tendon). Position of pivot shown by star in C. (A) Protracted position (50° to the longitudinal body axis). M1–2 is almost in line with M17–18, and its tendon (dashed line) is wrapped around the articulating peg. These muscles operate here with little mechanical advantage. The line of action of the RS muscle M3 offers greater mechanical advantage, and this muscle initiates the RS movement. (B) Mid-retraction (90°). The M1–2 tendon has unwrapped from around the peg. The resolved force will depend on the extent to which the contraction of M17–18 causes movement away from the pivot point (not shown here). (C) Retracted position (150°). The M1–2 tendon has moved away from the peg, offering greater mechanical advantage, while M17–18 has become unloaded.

Observations have been made on freshly dissected preparations to determine the mechanical relationships of the musculoskeletal system. As the basipodite is moved through its powerstroke arc, PS muscle M7–8 becomes unloaded before M4–6, indicating that it contributes only to the initial phase of movement. The RS muscles are also segregated in their action. As the returnstroke begins, M3 produces a large turning moment to initiate the movement (Fig. 2A). M1–2 will have little mechanical advantage at this stage, as its lines of action both through the tendon and through M17–18 lie precisely over the pivot formed by the peg. The resolved direction of force exerted by this muscle system will, however, depend on the effect of the contraction of M17–18, which will tend to pull the tendon away from the pivot, and thus increase the mechanical advantage. As movement progresses, M3 undergoes a rapid unloading, as does M17–18 beyond the mid-range of movement (Fig. 2B). However, from this point the mechanical advantage of M1–2, acting through its tendon attachment to the medial coxopodite, increases steadily as its line of action moves away from the pivot (Fig. 2C).

The swimmeret contains four other groups of muscle bundles: M16+19–26, M11–12–14–15, M13 and M9–10. The first group is concerned with closing, opening and curling the rami, and was not investigated in this study (but see Davis, 1968*b*). M11–12–14–15 lies in the basipodite and attaches onto the medial coxopodite (Figs 1B, 3A). M13 lies parallel with M11–12–14–15 but has its own

sclerite in the posterior articulation membrane. It is a lateral powerstroke muscle. The basipodite twisting muscles M9 and M10 share a common origin on the posterior–medial surface of the sternal rib socket (Fig. 3B). M10 crosses the joint diagonally to insert on the lateral basipodite wall, just ventral to the M13 sclerite. M9 inserts on the anterior cuticular rim of the basipodite, medial to the M13 sclerite (Fig. 3A). Between M9 and M10, and sharing their origin, is an elastic strand (strand B of Davis, 1968*b*) which inserts just lateral to M9 on the basipodite rim (Fig. 3B). There is also a second, shorter length of elastic tissue which originates from the lateral bundle of M10 and inserts at a more ventral location on the sternal rib cuticle. The anatomy and physiology of the receptor structures associated with these strands is described in the succeeding paper (Miyan & Neil, 1986).

If the rami are removed, and the muscles are viewed through the cut end of the basipodite, it can be seen that M9 acts across the pivot formed by the peg and hook of the swimmeret joint, and so would be capable of initiating the lateral twist (Fig. 3B). M10 lies more nearly over this joint, and its line of action will move away from the pivot only when lateral twisting is initiated. M13 may also contribute to this initial

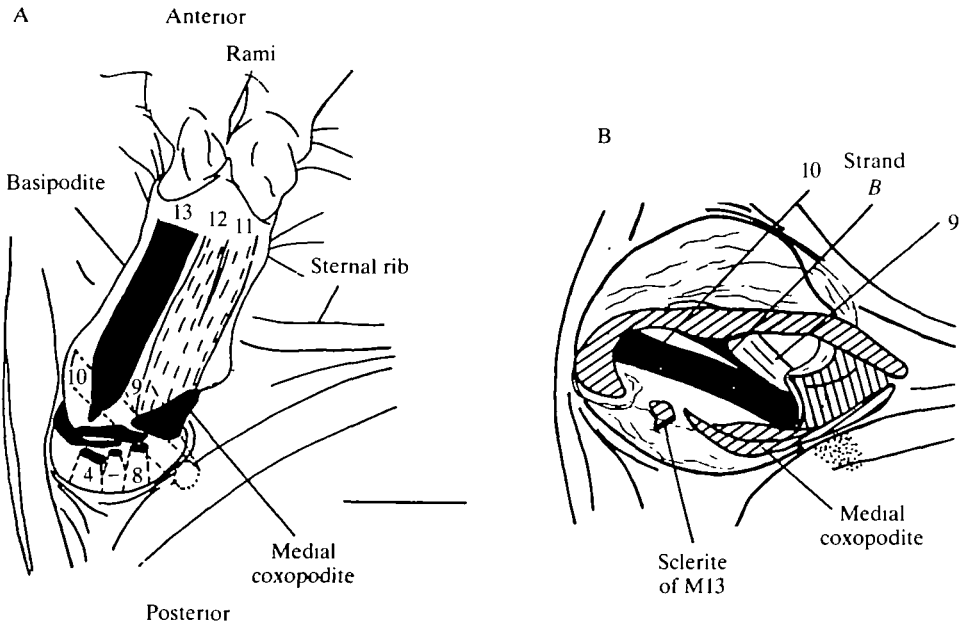

Fig. 3. (A) Posterior view of right ($N = 3$) swimmeret of *Nephrops* showing the insertions of the powerstroke (PS) muscles. The main PS muscles, M4–8, insert on individual sclerites embedded in the posterior articulating membrane. M11–12–14–15 (bundles 14–15 are overlain by bundles 11–12) runs from an origin on the medial coxopodite and M13 runs from an origin on a sclerite to insert alongside each other in the distal basipodite. The outlines of the twisting muscles M9 and M10 are included to show their relationship to the other PS muscles. (B) Ventral view of the right swimmeret to show the location of M9 and M10 spanning the abdominal–coxal–basal joint, and their relationship to the medial coxopodite and the sclerite of M13. An elastic strand (*B*) shares the origin with the muscle bundles, and inserts on the basipodite rim, laterally to M9. Scale bar: 2 mm (A); 0·8 mm (B).

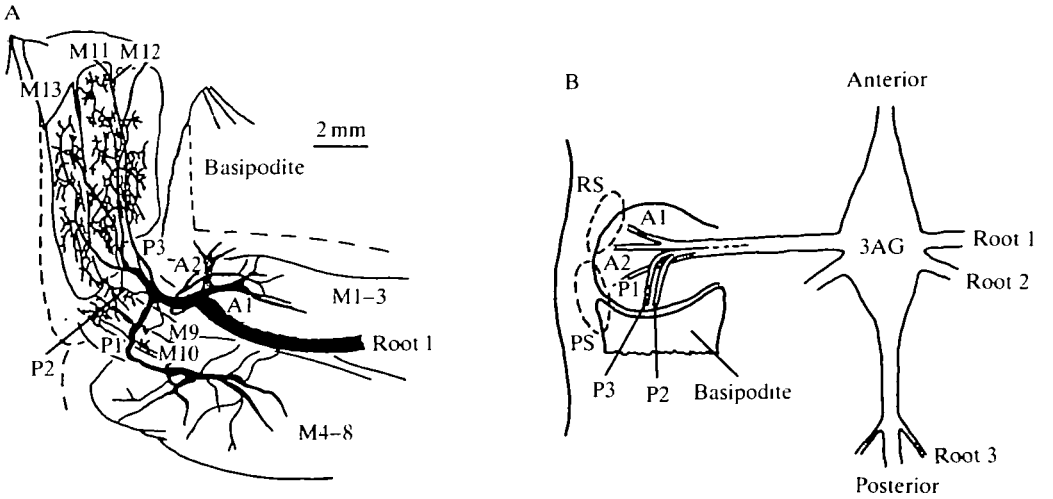

Fig. 4. Arrangement of the first abdominal nerve root which supplies the swimmeret of *Nephrops*. (A) *Camera lucida* drawing from a posterior aspect of the branches of the first root in the third right swimmeret, after staining with cobalt. The root divides into an anterior and posterior trunk. The anterior trunk subdivides into a dorsomedial A1 branch to the main returnstroke (RS) muscles M1–3, and a dorsolateral A2 branch (stippled) to the abdominal muscles and cuticular receptors. The posterior trunk subdivides into a dorsal P1 branch to the main powerstroke (PS) muscles M4–8 and to M9 and M10, a ventral P2 branch to PS muscles M11–12–14–15, M13 and M17–18, and a distal P3 branch to the rami. (B) Schematic drawing from a ventral aspect of the main branches of root 1 leaving the third abdominal ganglion (3AG) to supply the right swimmeret. Dashed outlines indicate the positions of the main PS and RS muscles.

rotation, since it can act through its sclerite in the posterior articulation membrane to alter the geometry of the coxal hook relative to the peg, and thereby increase the mechanical advantage of both M9 and M10. In contrast, the action of M11–12–14–15 would not produce this effect, since it acts directly on the medial coxopodite to pull the hook medially around the peg, thus preventing any change in the line of action of M9 and M10. These considerations suggest that an overt twisting movement of the basipodite might be expected only during active swimmeret beating, and not during tonic postural movements.

Innervation of the swimmeret

Each swimmeret is innervated exclusively by the ipsilateral first nerve root from the corresponding abdominal ganglion (Fig. 4A). This root is made up of two main trunks of nerve fibres, each of which contains both large diameter (>50 μm) and small diameter (<1 μm) fibres. The posterior trunk contains more fibres in total, and a higher proportion of small diameter fibres than the anterior trunk. Centripetal and centrifugal cobalt fills were carried out from the cut ends of different branches of these abdominal first nerve roots. There is a general, but incomplete, segregation of motor axons into an anterior trunk returnstroke muscle supply and a posterior trunk powerstroke muscle supply. The anterior trunk does not branch until well into the swimmeret, at which point it divides, sending a dorsomedial branch to the main

returnstroke muscle bundles (M1–3), and a dorsolateral branch to the abdominal musculature and sensory hairs of the lateral abdominal wall (Fig. 4B). A small ventral branch supplies the swimmeret muscle M17–18 and some of the closer and uncurling muscles of the rami. The posterior trunk separates before entry to the swimmeret and gives rise to three branches, which can be recognized in histological cross sections by their characteristic complements of large and small fibres. The posterior–dorsal branch innervates the main powerstroke muscle bundles M4–8, and small branches also innervate the twisting muscles M9 and M10. The other two branches of the posterior root enter the swimmeret basipodite, a ventral one giving rise to the innervation of M11–12–14–15, M13 and M17–18, and another proceeding into the rami. Two large diameter fibres are shared between the posterior ventral and the posterior dorsal branches, the latter supplying the powerstroke muscles M4–5. In addition to these motor fibres, the posterior trunk also carries the sensory innervation of the various swimmeret receptor systems, including two fibres with central cell bodies which supply the twisting muscle receptor (TMR) associated with M10 (Miyan & Neil, 1986).

Retrograde cobalt and cobalt/nickel differential fills from the central cut ends of the first root at its branch point proximal to the swimmeret demonstrate that there are two distinct groups of somata in the ventral rind of the ganglion: an anterior group of approximately 35 cell bodies and a posterior group of 20–25 cell bodies (Fig. 5A). A striking feature of the central fills is the staining of two distinct fibre tracts running dorsally across the ganglion (Fig. 5B). Separate cobalt fills of anterior and posterior root fibres show that there is a strong correspondence between the root of exit and the transganglionic projection, the only exceptions being a few fibres in the posterior root which send processes to the anterior transganglionic tract. These tracts originate from a mass of dendritic arborizations medial to the entry of the first root, and appear to terminate in discrete areas of arborization at the midline (mainly the anterior tract), or in the contralateral hemiganglion.

An additional feature demonstrated by intensification of the cobalt stain is the presence of projections from stained neurones both anteriorly and posteriorly out of the ganglion (Fig. 5C). Up to four fibres have been identified, and at least one cell body gives rise to projections in both directions. One of the anterior fibres is known to be a projection of a sensory neurone from the TMR (Miyan & Neil, 1986). Differential cobalt/nickel fills of anterior and posterior nerve roots show that two anterior fibres and a posterior fibre originate from the posterior group of cell bodies, while a third anterior fibre originates from the anterior group of cell bodies. All the anterior fibres have been traced as far as the adjacent ganglion, which makes it possible that they are involved in the intersegmental coordination of swimmeret beating.

Motor activity in swimmeret muscles

The pattern of motor activity seen in the swimmeret muscles of *Homarus* has been summarized by Davis (1969) and by Cattaert (1984). A similar pattern was seen in

Nephrops. In the absence of swimmeret beating there was tonic activity in the RS muscles, but the main PS muscles were silent. When beating occurred there was alternating activity in the main PS and RS muscle groups of each swimmeret (Fig. 6A), with tight coupling between bilateral partners (Fig. 6B) and an anterior wave of excitation between segments (Fig. 6C). PS muscle M11–12–14–15 was strongly activated in rearward beating, but M13 was only weakly activated, as were M9 and M10.

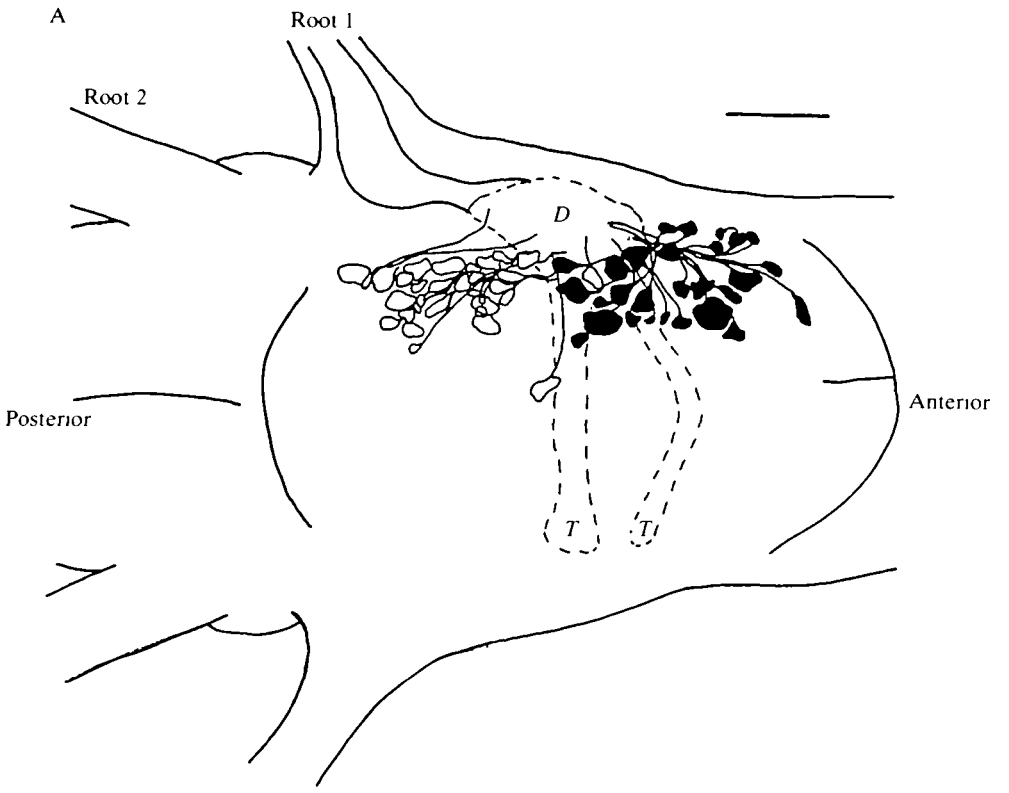

Fig. 5. (A) *Camera lucida* drawing of the third abdominal ganglion, viewed ventrally, following differential cobalt/nickel staining of somata supplying axons to the anterior trunk (filled outlines) and the posterior trunk (unfilled outlines) of the first root. All the somata are ipsilateral to the root, and with the exception of those unfilled outlines within the anterior group, they are segregated into an anterior group supplying axons to the anterior trunk, and a posterior group supplying axons to the posterior trunk. There is a dense mass of dendritic endings (*D*) between the entry of the fibres to the ganglion and the somata. Two fibre tracts (*T*) emerge from the dendritic mass to traverse by dorsal routes to the other side of the ganglion. Scale bar, 200 μm. (B) A dorsal view of the third abdominal ganglion following a cobalt backfill of the whole first root on the right side (*r1*), showing the fibre tracts emerging from the dense neuropilar region. Scale bar, 200 μm. (C) Intensified cobalt fill of root 1 to the third abdominal ganglion. The preparation has been orientated to display the projections of certain fibres along the cords. One soma (*1s*) has continuity with both an anterior-going fibre (*1A*) and a posterior-going fibre (*1P*). Two other anterior fibres can be seen (*2*, *3*), and also a paired projection of two fibres which loops out posteriorly and returns to the ganglion (*L*). *A*, anterior; *V*, ventral. Scale bar, 100 μm.

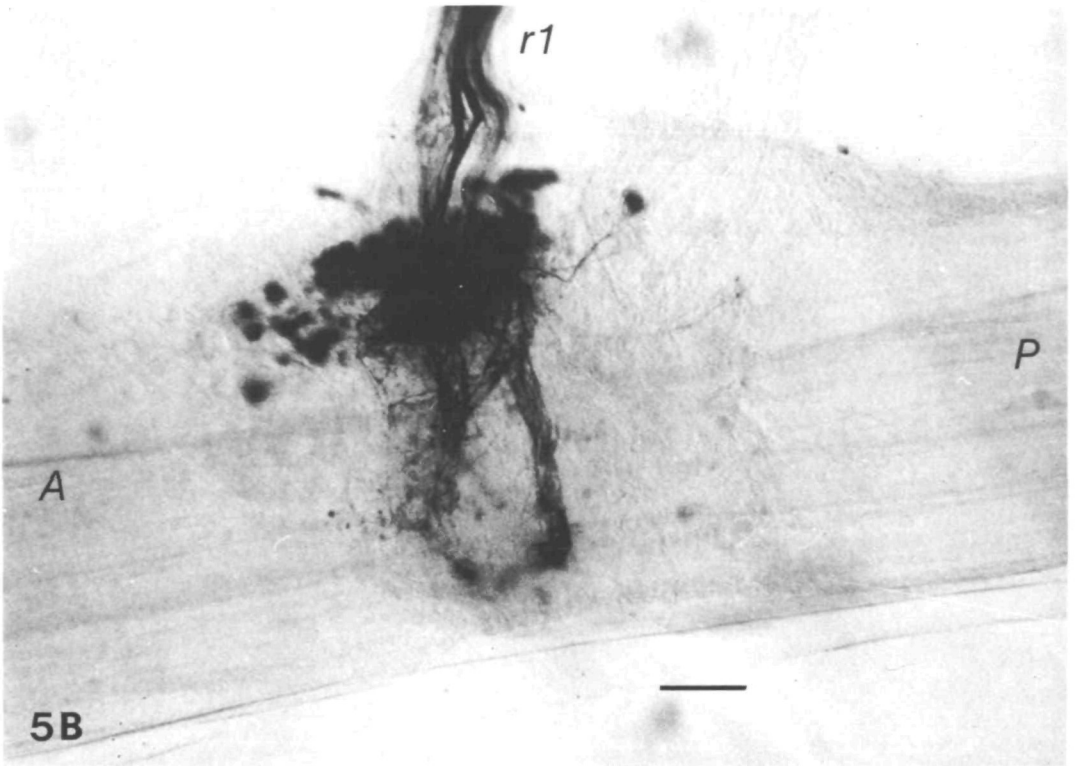
r1
P
A
5B

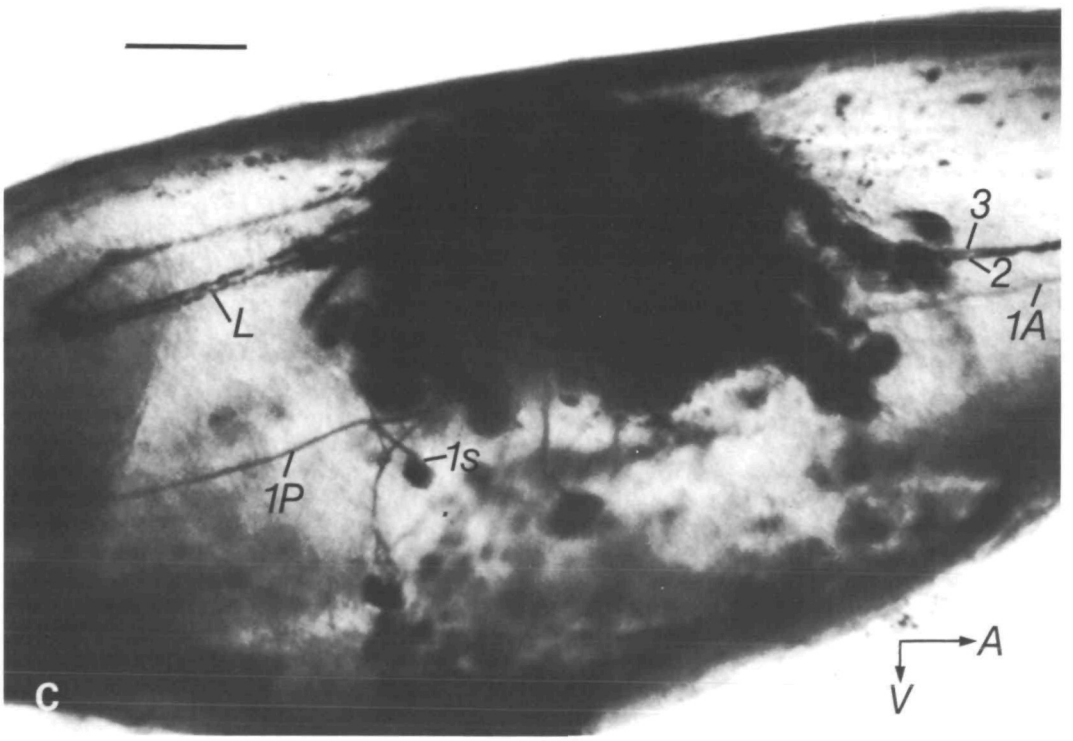
3
2
1A
L
1s
1P
A
V
C

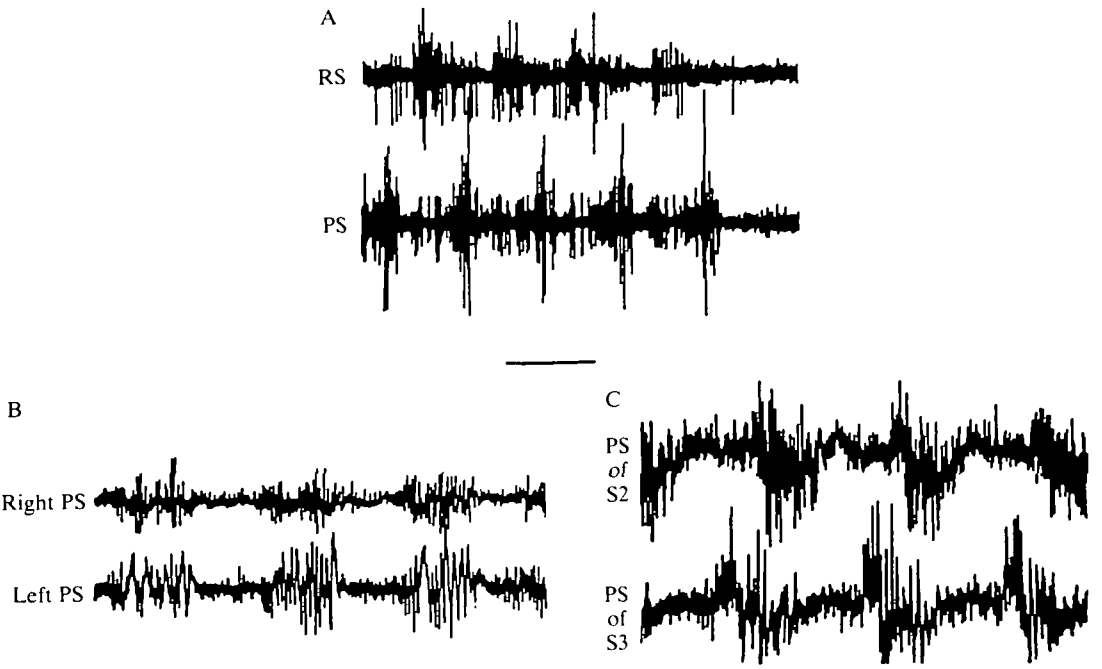

Fig. 6. Muscle activities in swimmeret beating, recorded myographically. (A) Powerstroke (PS) and returnstroke (RS) muscles from one swimmeret, showing alternating pattern. (B) PS muscles of the right and left swimmerets of one segment, showing synchrony. (C) PS muscles of the left swimmerets 2 and 3, showing the segmental delay in the anterior-going metachronal wave. Time bar, 0·4 s (A); 0·2 s (B,C).

Tilting a quiescent animal about its longitudinal axis by as little as 5° acted as a powerful stimulus to initiate swimmeret beating, although the form of the beat was somewhat modified. The swimmerets on the side tilted upwards beat laterally, producing a righting torque, while the swimmerets on the downward side beat weakly rearwards, or in many cases ceased beating altogether. This bilateral uncoupling was a consistent feature of tilted beating, whereas in the upright animal, coupling was always strictly observed between the two swimmerets of one segment. Activity in the main PS muscles was essentially unaltered when rearward beating changed to lateral beating. However, of the other members of the powerstroke group, M11–12–14–15 was silent in lateral beating, whereas M13, M9 and M10 discharged strongly. RS muscles also displayed tilt-related activity. We have looked in detail at the nature of these muscle activities which are specifically modulated by tilt stimuli.

The twisting muscles M9 and M10

Since nothing is presently known about the electrical activity of M9 and M10, and since this information is necessary to interpret their responses to tilt stimuli, an intracellular study of these muscles was undertaken. M9, which is a single bundle of fibres with average sarcomere length of 10 μm, receives three or four motor axons. In the absence of specific stimuli, M9 received a continuous train of tonic input from

two units which could be identified in extracellular recordings from the dorsal posterior root (Figs 7A, 8B). M10, which is composed of a separate medial bundle (fibre sarcomere length 7 μm) and lateral bundle (fibre sarcomere length 5 μm), received at least six axons (Fig. 7B). Fibres in the medial bundle of M10 showed a tonic activity similar to those of M9, but the lateral bundle of M10 was usually silent. Periodically M9 tonic activity increased, and at these times there were also bursts in the lateral M10 bundle. Simultaneous penetrations of fibres in the two muscles demonstrate these marked differences in their activities (Fig. 7C).

The tonic activity to M9 and the medial M10 bundle was modulated by various mechanosensory stimuli, such as brushing the cephalothorax and squeezing the uropod. No other muscles of the PS group were affected in this way by stimuli subthreshold for eliciting swimmeret beating. The most effective and repeatable effect, however, was produced by imposing a roll tilt to the body. In cases where this stimulus did not elicit swimmeret beating, M9 and the medial M10 bundle were tonically excited in the 'side-up' swimmerets, and inhibited in the 'side-down' swimmerets. This was demonstrated using myogram recordings (Fig. 8A), nerve recordings from the posterior dorsal root, and by intracellular muscle recordings (Fig. 8B) in association with body tilts, or in some cases tilting of the isolated 'head' of the animal (Miyan, 1984). Since it is most convenient to carry out these experimental procedures (except myographic recordings) using an inverted preparation, the tilt responses which occur around the inverted position were compared with those around the upright position. Histograms obtained from ten cycles of body oscillation through $\pm 45°$ of each of these positions were similar in form, confirming that the response is symmetrical about the upright and inverted positions (Fig. 9A). However, around the upright position the peak is sharp, whereas around the inverted position it forms a plateau.

Using such sinusoidal tilt stimuli it was shown that, in the absence of beating, activity in the tonic medial bundle of the twisting muscle M10 (and also, not shown, M9) had a consistent and precise point of onset, at 25° before the upright body position, approached from side-down (arrows in Fig. 9A). This initiation point was independent of stimulus frequency over the range tested (Fig. 9B), although the peak response and response termination varied more widely with frequency. In most cases, however, tilting induced swimmeret beating, and the activity of the medial M10 bundle in the upward swimmerets was then switched from a tonic pattern to one in which bursts of activity occurred at times corresponding to the powerstroke movements, with inhibition during the returnstroke (Fig. 10). It seems that under these circumstances M10 is influenced powerfully by the central pattern generator (CPG) for swimmeret beating.

A side-symmetrical pattern of lateral beating was commonly seen when the animal was tilted to each side of the upright. This was shown in the recordings from the lateral M10 bundles of both swimmerets, but also involved similar phasic activation of the medial M10 bundle, and M9 (Fig. 10A). However, another frequently encountered relationship was one in which lateral swimmeret beating was induced by a tilt to one side, but no beating by a tilt to the other side (Fig. 10B). In Fig. 10B, this

is reflected in the strong tonic activity of the medial M10 bundle, and in the phasic activity of the lateral M10 bundle. Although in the side-down swimmeret there was more often an inhibition of medial M10 activity, in some cases small bursts appeared in antiphase with PS activity in the contralateral swimmeret (Fig. 10C,D). The initiation of beating activity occurred at an angle closer to the upright body position than that for tonic activity, and this initiation point remained consistent on successive tilts. Moreover, motor activity commenced each time at exactly the same

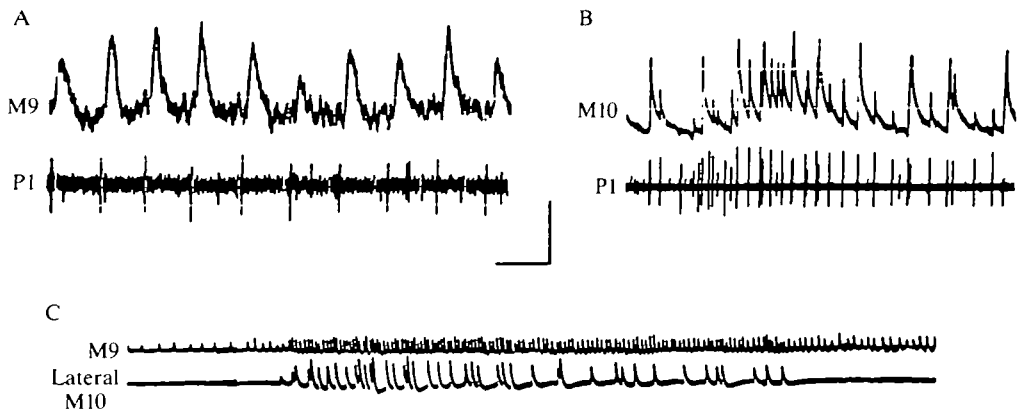

Fig. 7. Intracellular recordings from the swimmeret twisting muscles. (A) M9. Correlation of the recorded EPSP with firing of a spontaneously active unit in the P1 branch of the first abdominal nerve root. (B) M10. Correlation of several sizes of EPSP with evoked activity of different units in the P1 branch of the first root. (C) Simultaneous penetration of fibres in M9 and the lateral bundle of M10, demonstrating the periodically increased tonic activity of at least two EPSPs in M9 which is accompanied by activity in M10. Scale bars, 0·2 s and 2 mV (A); 2·0 s and 5 mV (B); 1·0 s, and 6 mV for M9 and 12 mV for M10 (C).

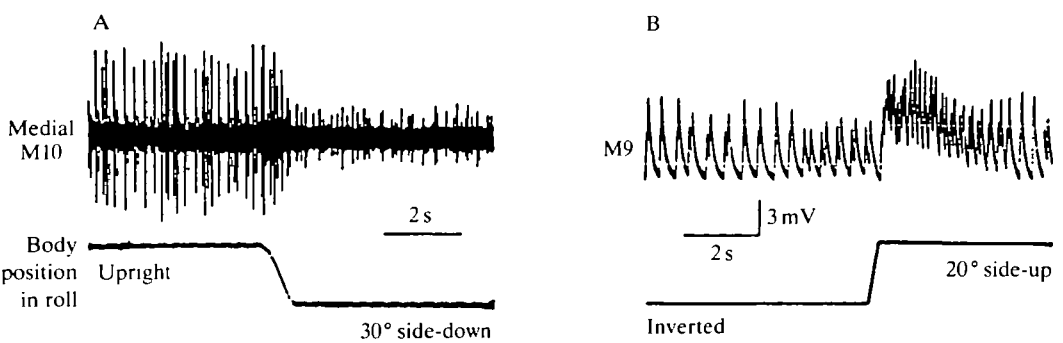

Fig. 8. Activity of the twister muscles in relation to statocyst stimulation. (A) Myogram recording from the medial M10 bundle in the left swimmeret while the animal was held initially upright, then tilted 30° side-down (ramp). (B) Intracellular recording from a fibre of M9 in the left swimmeret while movement is imposed upon the isolated 'head' (see Materials and Methods). In the initial inverted position there is tonic activity involving two EPSPs which fire at slightly different frequencies and show degrees of summation. When the 'head' is tilted by 20° in a direction equivalent to left-side-up from the upright there is an increase in the firing frequency of both units.

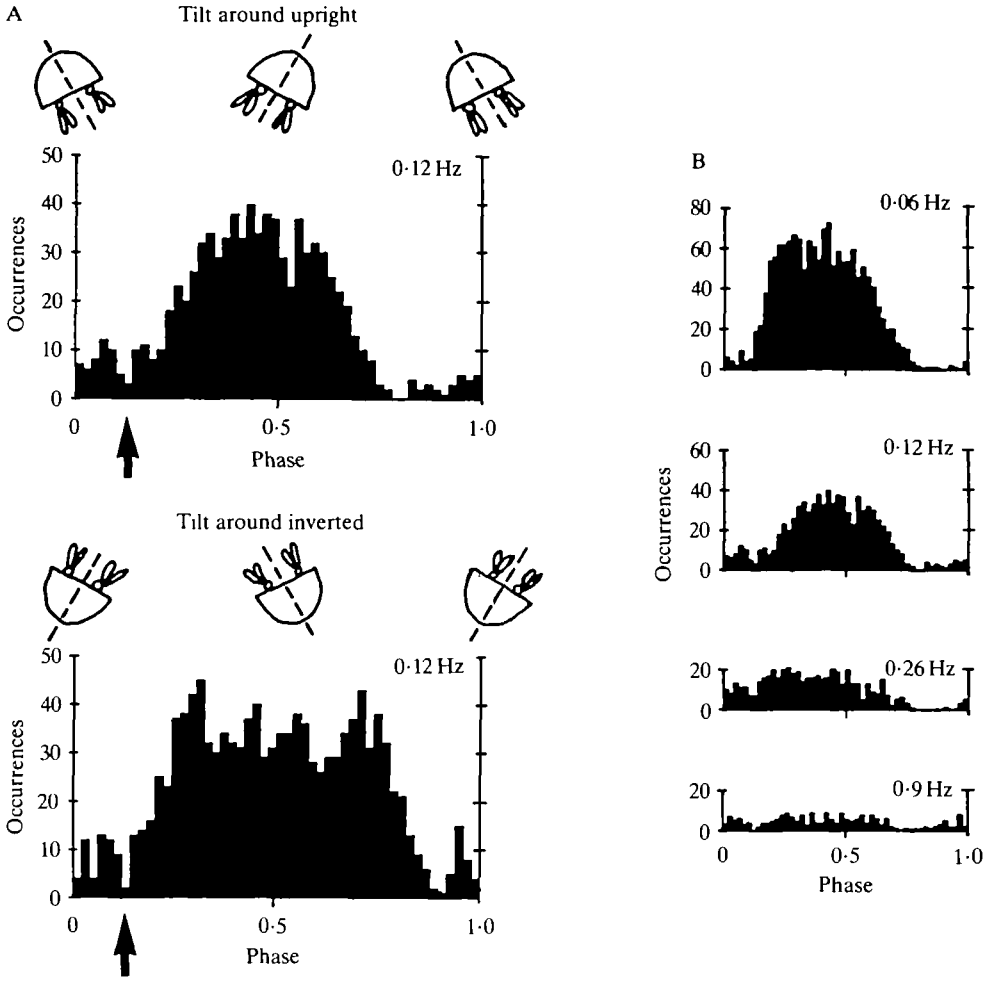

Fig. 9. Phase histograms of the myographic activity of the M10 medial bundle in the left swimmeret in response to 10 cycles of sinusoidal body tilts of ±45° around the upright (or inverted). A cycle is defined between successive extreme right-side-up positions. (A) Comparison of tilts around the upright (upper histogram) and inverted (lower histogram) body positions. For the inverted test the animal was turned in a roll through 180° before applying the same movements as for the upright test. Excitation begins at 25° before the upright (or inverted) positions, as indicated by the arrows. Cycle frequency, 0·12 Hz. (B) Comparison of tilts around the upright position at different frequencies, demonstrating the phase stability of the response.

phase position in the swimmeret beat cycle. The precision of this phase relationship is reflected in plots of the accumulated activity from successive cycles of stimulation, in which individual peaks corresponding to each beat can still be recognized (Fig. 10D).

The lateral powerstroke muscle, M13

The activation of this phasic PS muscle was studied in relation to the frequency and range of the body tilt stimulus. The onset of bursting discharge in the upwardly

moved swimmeret occurred very precisely around the upright position (Fig. 11A). The number of beats completed within the sensitive range of movement necessarily varied with the frequency of tilt, but the beat frequency itself remained fairly constant. The precise positional relationship of response onset and the constancy of beat frequency are demonstrated, as for M10, in the accumulated phase histograms of activity (Fig. 11B). This was further demonstrated by commencing oscillatory

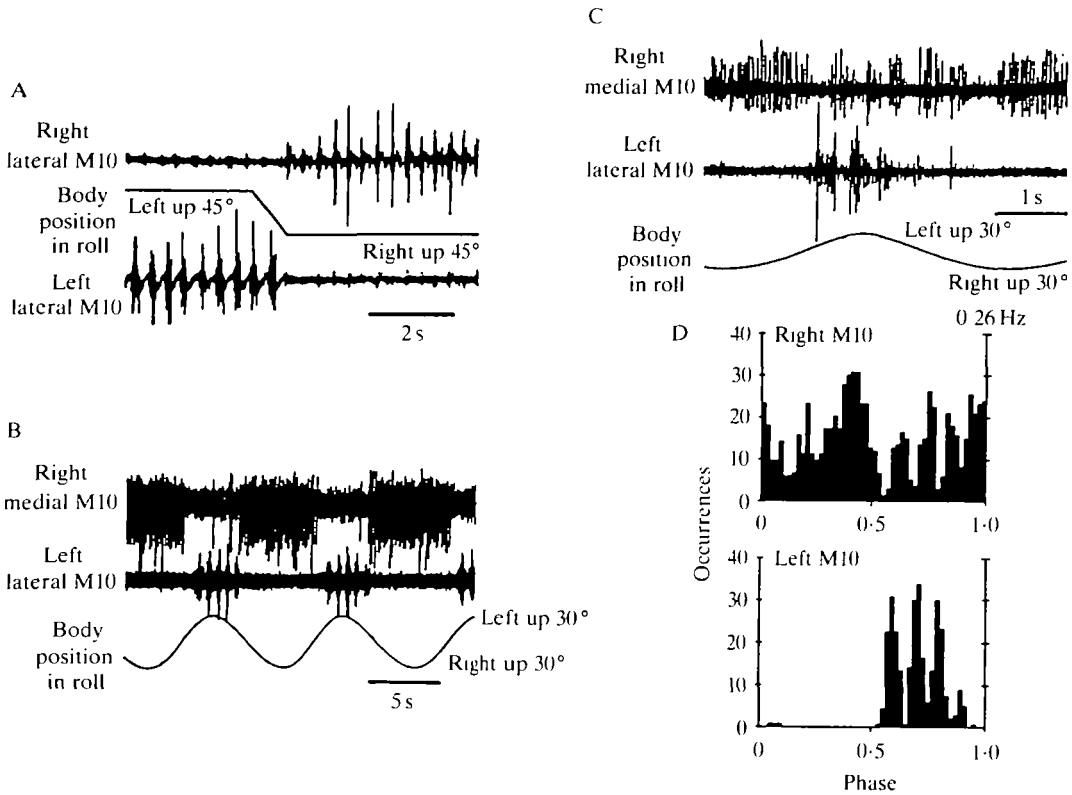

Fig. 10. Bilateral relationships in the activity of twisting muscle M10. (A) Records of activity from the lateral bundle of M10 in the right and left swimmerets during body tilt from 45° left-side-up to 45° right-side-up, when there is swimmeret beating. There is a coincidence of the termination of beating in the left swimmeret with the initiation of beating in the right swimmeret precisely at the upright body position. (B) Records from the right medial M10 and left lateral M10 bundles during sinusoidal tilts from 30° left-side-up to 30° right-side-up. In this case tilt to left-side-up induces beating and M10 bursting in the left swimmeret, but tilt to right-side-up induces no beating and only tonic M10 activity in the right swimmeret. Note that the gain on the upper trace is greater than that on the lower trace. (C) Records as in B (on a faster time base) from another preparation which shows bursting in M10 of the right swimmeret on left-side-up alternating with the M10 bursts (and powerstroke, PS, movements) of the left swimmeret. (D) Phase histograms from the records shown in C collected over 10 cycles of tilt at a frequency of 0·26 Hz. A cycle is defined between extreme right-side-up positions. M10 beating activity in the left swimmeret coincides with periods of depressed M10 activity in the right swimmeret. This should be compared with the strict coupling observed across segments in PS activation during rearward beating (e.g. Fig. 6B).

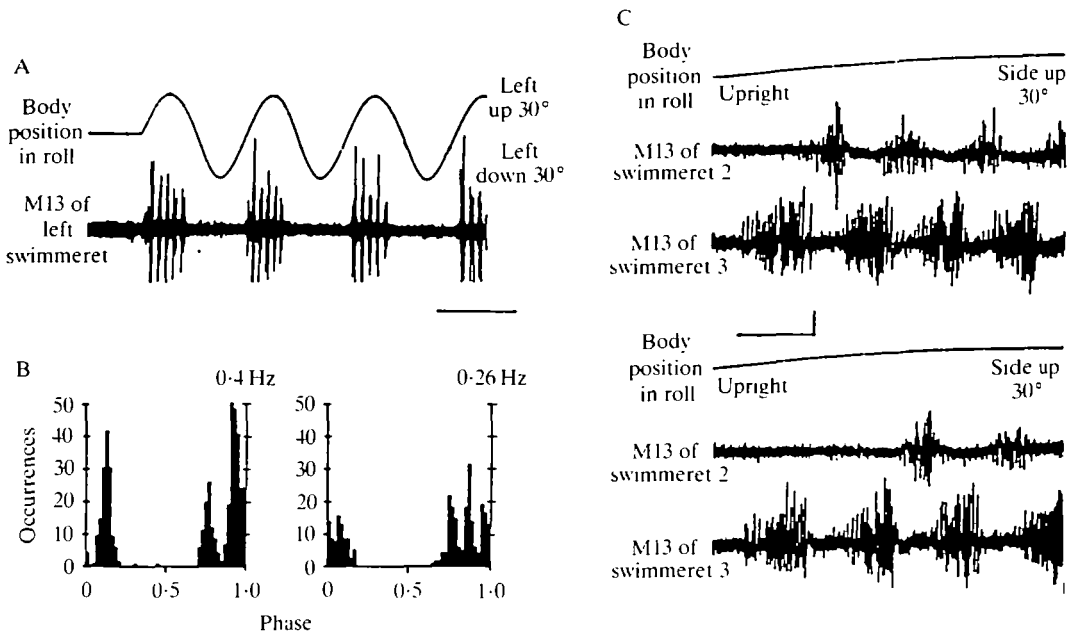

Fig. 11. (A) Activity of the lateral powerstroke muscle M13 in the left swimmeret ($N = 3$) during sinusoidal body tilts of ±30° at 0·2 Hz. Lateral beating, which involves M13 bursts, is initiated close to the upright position approached from side down. (B) Phase histograms, obtained from the same preparation, of accumulated activity of M13 over 10 cycles of body tilt at 0·26 Hz and 0·4 Hz. A cycle is defined between extreme left-side-up positions. The point of onset of activity remains constantly around the upright (i.e. 0·75 phase position) and bursting activity from successive cycles is superimposed to form sharp phase peaks. The number of these peaks decreases with increasing frequency of tilt, reflecting a relatively constant rate of beating. (C) Activity of M13s in left swimmerets 2 and 3 during sinusoidal body tilts, showing the effect of the excitation level on recruitment. In the upper panel, M13 of swimmeret 3 is activated just beyond the upright (beginning of trace), and M13 of swimmeret 2 is recruited with an appropriate metachronal delay. In the lower panel, when the animal is at a lower excitation level, no burst occurs in 2 following the first burst in 3, but activity subsequently begins at the second appropriate interval. Scale bars, 4 s (A); 0·5 s and 30° (C). Up on movement traces = left side up.

tilts from different initial angles, and at different frequencies. In all cases the initiation of beating occurred at the upright body position, irrespective of the initial position or the velocity of movement.

Simultaneous recordings from the M13s of all swimmerets demonstrated the intersegmental relationships in lateral beating. These were similar to those for rearward beating, with a rear-to-front progression of PS activation. Beat frequencies, at 1–2 Hz, were generally higher than those in rearward beating, and segmental delays were 100–200 ms. The onset of lateral beating, as of rearward beating, also showed a rear-to-front progression, and indeed only the more posterior swimmerets were activated at low levels of 'arousal'. If excitability was increased, either by non-specific stimulation or by tilting itself, the more anterior swimmerets were recruited with appropriate time delays relative to the first beat of a more posterior swimmeret

(Fig. 11C). At intermediate levels of excitability an anterior swimmeret might not be recruited into the first beat, but would be incorporated at a second or later appropriate interval (Fig. 11C). This is most probably due to the increased stimulation produced by further tilting.

The returnstroke muscles

Tonically active units of the RS muscles maintain the swimmerets in a fully protracted resting posture. Recordings from the RS muscles showed that these units also had a tilt-related response, even in the absence of beating. In the side-up swimmeret they showed increased discharge which accompanied the increased activity of lateral twisting muscles. The corresponding reduction in RS activity in the side-down swimmeret resulted in sagging of the appendage from its fully protracted position. When beating was initiated, the RS muscles showed bursting on the up side, which alternated with the PS discharges of the same swimmeret (Fig. 12). The tonic RS units, unlike the tonic M9 and M10 units, appeared to be unaffected by this bursting drive, and fired continuously throughout the sensitive range. The range of tilts over which the phasic beating was active was more restricted than that for the tonic response, and again lay precisely from the upright body position towards the side-up position. The reactions of the RS system to tilt are, however, less consistent than those of the twisting muscles, suggesting that they are, in addition, influenced by other variable inputs.

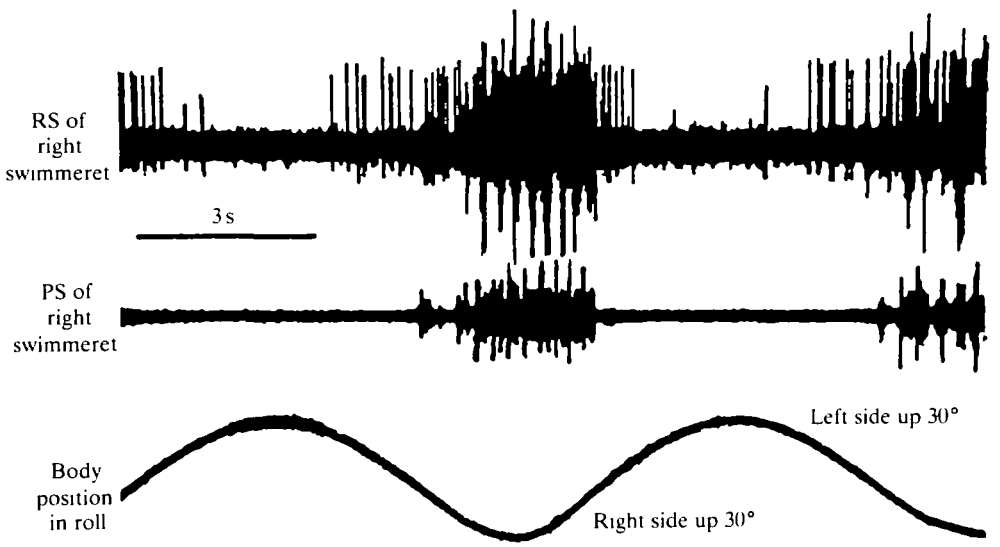

Fig. 12. Myogram recordings from the returnstroke (RS) and powerstroke (PS) muscles of a right swimmeret during sinusoidal tilts of ±30° at 0·12 Hz. Swimmeret beating occurs when the body is tilted right-side-up, and there are alternating bursts in the phasic RS and PS units. A section of this record is shown on a faster time base in Fig. 6A. In addition, a tonic RS unit begins firing earlier on the approach to side-up, and continues firing through the side-up range.

DISCUSSION

The swimmeret skeletomuscular system has several mechanical specializations. The single articulation about the peg and hook allows both fore and aft movement, and also lateral rotation. In addition, it contributes to the fractionation of muscle activities in the RS movement, by serving as a pulley around which the tendon of M1–2 operates. This arrangement prevents M1–2 from producing retraction forces, since its line of action cannot pass over the pivot point. During the first part of the RS movement, the tendon insertion of M1–2 describes an arc, so that there is no external shortening of the muscle, but also little protraction force as the muscle has no mechanical advantage. However, the tension accumulated during this stage will act with increasing mechanical advantage through the second part of the movement, and ensure that the RS is driven to completion. In this respect the system could be acting as a power amplifier, with the energy being stored either in the muscle itself, or in the elastic material of the tendon. A similar mechanism has been described by Ellam (1978) in the coxal muscles of the crab claw, which enables the animal to execute a rapid defensive strike.

As a result of the mechanical relationship of M10 to the basal articulation in the swimmeret, its contractions will have little effect without the initial twisting produced by M9 contractions. This arrangement is reflected to some degree in the differences between the two muscles. According to the properties of crustacean muscles described by Atwood (1967, 1973), M9, with long sarcomeres and tonic activity, is probably a powerful, slowly fatiguing muscle, while M10, with a lateral bundle of short sarcomeres and a medial bundle of intermediate length sarcomeres, has the properties of a phasic and rapidly fatiguing muscle.

It is known that statocyst information in *Nephrops* is conveyed to abdominal motor systems by a small number of descending interneurones (Miyan, 1982; D. M. Neil, unpublished observations). More detailed information is available for the crayfish, in which four pairs of interneurones collect selectively from statocyst receptors coding restricted angular ranges, and reflect the body position of the animal in their tonic firing levels. They pass by ipsilateral and contralateral routes as far as the terminal abdominal ganglion, where they make parallel mono- and polysynaptic connections onto the premotor circuits to the uropod motoneurones (Takahata & Hisada, 1982; Takahata, Yoshino & Hisada, 1985). It is probable that similar circuits are also presynaptic to swimmeret motoneurones (Heitler, 1983). Although our data provide no direct evidence about the neuronal identity of premotor elements, they enable us to predict the types of connection which must necessarily exist between statocyst interneurones, the swimmeret oscillator and the swimmeret motoneurones to produce the observed phase-related activity of swimmeret muscles in lateral beating.

A model which incorporates all these features places descending statocyst interneurones both in series and in parallel with the swimmeret CPG (Fig. 13). Since tilting the body has such a strong and consistent influence on the initiation of swimmeret beating, statocyst interneurones must act as a gate for CPG expression. General mechanosensory stimuli and specific postural actions, notably loss of leg

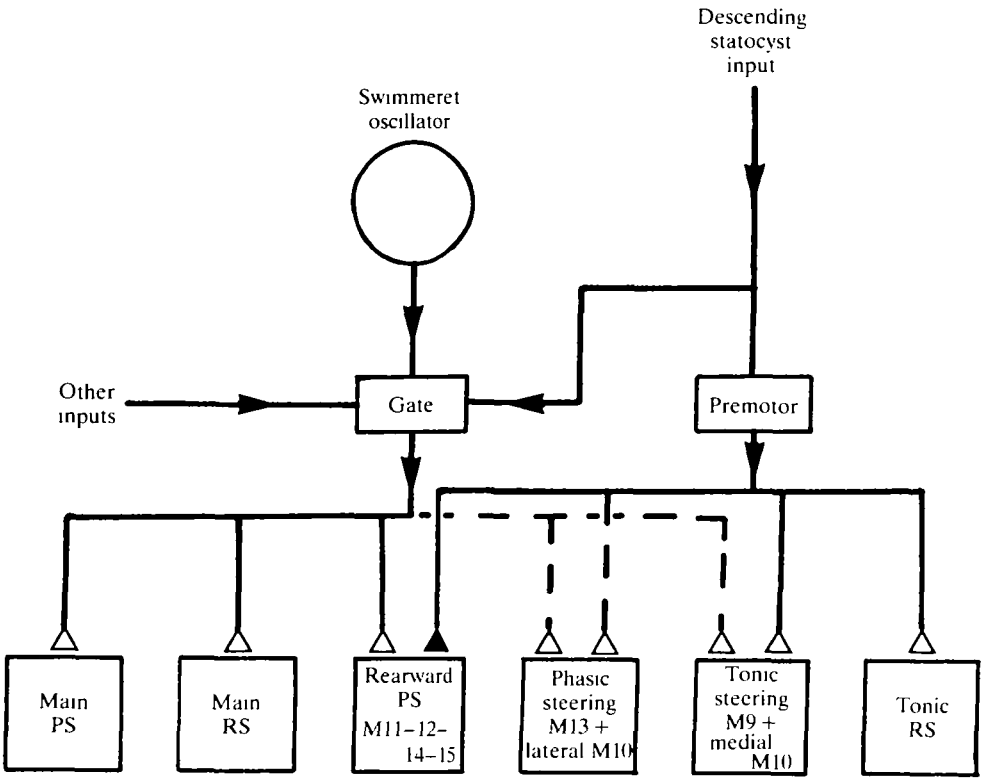

Fig. 13. Block diagram of the possible functional interconnections between the descending statocyst input and the swimmeret central pattern generator which together control the activity of the different swimmeret muscles. Rectangles represent premotor circuits, open triangles excitatory influences, closed triangles inhibitory effects, and dashed lines subthreshold effects. RS, returnstroke; PS, powerstroke. Details in text.

contact with subsequent abdominal extension (Larimer & Eggleston, 1972; Takahata, Yoshino & Hisada, 1981) and locomotion (Cattaert & Clarac, 1983), are also known to act in this way. Since no changes are observed in the basic PS/RS pattern of the swimmeret in tilted beating, this gating effect is the major modulatory influence of the statocyst interneurones on the main PS and RS muscles. Indeed, the alternation between lateral beating on side-up, and either rearward beating or a cessation of beating on side-down, is consistent with this conclusion.

Other swimmeret muscles appear to be influenced by descending statocyst interneurones in more complex ways. The lateral powerstroke muscle, M13, is incorporated into the beat cycle only when the animal is tilted side-up. Interaction of a CPG output which would have a subthreshold effect on M13 motoneurones, with a sustained synaptic drive from statocyst interneurones, would explain such a position-related effect. However, since M13 is silent when body tilt does not induce beating, it must be concluded that the direct pathway is also supplying subthreshold input. Only when the two subthreshold effects coincide, in tilted beating, do M13 motoneurones discharge. The phasic bundles of M10 also behave as if controlled by such an AND gate.

PS muscles which are silent in lateral beating must receive specific inhibitory inputs during body tilt, either from statocyst interneurones themselves, from their immediate postsynaptic circuits, or possibly by recurrent inhibition from lateral PS motoneurones. There is also some evidence that peripheral inhibitory neurones are involved (Davis, 1969).

M9 and the medial bundle of M10 clearly reflect direct drive from statocyst interneurones, since they show tonic tilt-related behaviour in the absence of swimmeret beating. When beating occurs, however, they are entrained to the CPG, and therefore must also be postsynaptic to this oscillator circuit. The gating effect is phase dependent, since the twisting muscles are activated only during the PS.

The difference in onset of tilt-related activity under these two conditions suggests that the statocyst signal is in some way used to define two distinct set points. There is no obvious basis for this in the anatomy of the statocyst itself (Newland, 1985), or in the discharge patterns of individual statocyst interneurones (Miyan, 1982). It is more likely to reflect differences in threshold firing levels of the different motoneurone pools to the statocyst signal. The threshold for tonic tilt activation must be lower in M9 and medial M10 (at interneurone firing levels corresponding to body tilts of 25° before the upright) than for phasic activation of M13 at 0°. This suggests that the statocyst interneurones and CPG converge onto different premotor circuits which are specific to particular groups of swimmeret motoneurones.

It is interesting to find muscles, particularly in the RS group, which are apparently uninfluenced by the CPG, and yet have tonic output which is powerfully regulated by statocyst interneurones. A few phasic RS motoneurones in the crayfish show a similar isolation from the CPG, although their responses to tilt are not known (W. J. Heitler, personal communication).

The model in Fig. 13 for the interaction of statocyst input with rhythmic motor output in the lobster swimmeret system has many features consistent with the recently described properties of local premotor non-spiking interneurones in crayfish abdominal ganglia (Heitler & Pearson, 1980; Heitler, 1983; Reichert *et al.* 1982; Takahata, Nagayama & Hisada, 1981; Nagayama, Takahata & Hisada, 1983; Paul & Mulloney, 1985*a*,*b*). This model may be generally applicable to other locomotor systems which involve both rhythmic propulsion and steering. Analysis of locust flight, in which many of the interneurones have been fully characterized (Robertson & Pearson, 1982), has led to similar conclusions about the mutual gating of exteroceptive input and oscillating CPG output (Reichert *et al.* 1985). The dual capacity of statocysts both to initiate and to modulate lobster swimmeret activity equates with the similar actions of wind-sensitive hairs on the locust flight system. However, a closer analogy in terms of course control exists between lobster statocysts and locust ocelli, since they perform the equivalent functions of detecting deviations relative to the field of gravity or the horizon, respectively. Descending ocellar interneurones make strong presynaptic connections onto thoracic interneurones, which are in turn both postsynaptic to the flight CPG and presynaptic to the flight motoneurones (Rowell & Pearson, 1983; Reichert *et al.* 1985). In consequence, the thoracic interneurones are powerfully modulated at wingbeat frequency and, in turn,

gate the ocellar signal so that the flight motoneurones receive input only at certain phases of the wingbeat cycle. Further investigations of the lobster swimmeret system at the level of local interneurones are required to determine if similar neuronal mechanisms underlie the control of lateral beating expressed when the animal is displaced from the upright.

This research was supported by an SERC Research Studentship No. 78309158 to JAM, and forms part of the Ph.D. thesis submitted to Glasgow University (1982).

REFERENCES

ALTMAN, J. S. & TYRER, N. M. (1980). Filling selected neurones with cobalt through cut axons. In *Neuroanatomical Techniques. Insect Nervous System* (ed. N. J. Strausfeld & T. A. Miller), pp. 377–400. New York, Heidelberg, Berlin: Springer.

ATWOOD, H. L. (1967). Crustacean neuromuscular mechanisms. *Am. Zool.* **7**, 527–551.

ATWOOD, H. L. (1973). An attempt to account for the diversity of crustacean muscle. *Am. Zool.* **13**, 357–378.

BACON, J. P. & ALTMAN, J. S. (1977). A silver-intensification method for cobalt-filled neurones in wholemount preparations. *Brain Res.* **138**, 359–363.

CATTAERT, D. (1984). Polymorphisme d'expression d'un système locomoteur vestigial chez le homard *Homarus gammarus*. These de 3° Cycle, Université de Bordeaux I.

CATTAERT, D. & CLARAC, F. (1983). Influence of walking on swimmeret beating in the lobster *Homarus gammarus*. *J. Neurobiol.* **14**, 421–439.

DAVIS, W. J. (1968*a*). Lobster righting responses and their neural control. *Proc. R. Soc.* B **170**, 435–456.

DAVIS, W. J. (1968*b*). Neuromuscular basis of lobster swimmeret beating swimmeret. *J. exp. Zool.* **168**, 363–378.

DAVIS, W. J. (1969). Neural control of swimmeret beating in the lobster. *J. exp. Biol.* **50**, 99–118.

ELLAM, L. D. (1978). A neurophysiological analysis of aggressive behaviour in *Carcinus maenas*. Ph.D. thesis, University of London.

HEITLER, W. J. (1983). The control of rhythmic limb movements in Crustacea. In *Neural Origin of Rhythmic Movements* (ed. A. Roberts & B. L. Roberts). *Symp. Soc. exp. Biol.* **37**, 351–382.

HEITLER, W. J. & PEARSON, K. G. (1980). Non-spiking interactions and local interneurones in the central pattern generator of the crayfish swimmeret system. *Brain. Res.* **187**, 206–211.

HISADA, M. & NEIL, D. M. (1985). The neuronal basis of equilibrium behaviour in decapod crustaceans. In *Co-ordination of Motor Behaviour* (ed. B. M. H. Bush & F. Clarac), pp. 229–248. Cambridge: Cambridge University Press.

HUGHES, G. M. & WIERSMA, C. A. G. (1960). The co-ordination of swimmeret movements in the crayfish, *Procambarus clarkii* (Girard). *J. exp. Biol.* **37**, 657–670.

LARIMER, J. L. & EGGLESTON, A. C. (1971). Motor programs for abdominal positioning in the crayfish. *Z. vergl. Physiol.* **74**, 388–402.

LOEW, E. R. (1976). Light, and photoreceptor degeneration in the Norway lobster, *Nephrops norvegicus* (L.). *Proc. R. Soc.* B **193**, 31–44.

MIYAN, J. A. (1982). The neuromuscular basis of the swimmeret equilibrium reaction in the lobster *Nephrops norvegicus* (L). Ph.D. thesis, University of Glasgow.

MIYAN, J. A. (1984). A method for the neurophysiological study of reflexes elicited by natural statocyst stimulation in lobsters. *J. exp. Biol.* **108**, 465–469.

MIYAN, J. A. & NEIL, D. M. (1986). Swimmeret proprioceptors in the lobsters *Nephrops norvegicus* L. and *Homarus gammarus* L. *J. exp. Biol.* **126**, 181–204.

NAGAYAMA, T., TAKAHATA, M. & HISADA, M. (1983). Local spike-less interaction of motoneurone dendrites in the crayfish *Procambarus clarkii* (Girard). *J. comp. Physiol.* **152**, 335–345.

NEIL, D. M. (1982). Compensatory eye movements. In *Biology of the Crustacea*, vol. IV (ed. H. L. Atwood & D. C. Sandeman), pp. 133–163. New York: Academic Press.

NEIL, D. M. (1985). Multisensory interactions in the crustacean equilibrium system. In *Feedback and Motor Control in Invertebrates and Vertebrates* (ed. W. J. P. Barnes & M. Gladden), pp. 277–298. London: Croom Helm.

NEIL, D. M., BARNES, W. J. P. & BURNS, M. D. (1982). Reflex antennal movements in the spiny lobster, *Palinurus elephas*. I. Properties of reflexes and their interaction. *J. comp. Physiol.* **147**, 259–268.

NEIL, D. M. & WOTHERSPOON, R. M. (1982). Structural specializations, fluid flow and angular sensitivity in the statocyst of the lobster *Nephrops norvegicus*. *J. Physiol., Lond.* **329**, 26–27P.

NEWLAND, P. L. (1985). The control of escape behaviour in the Norway lobster, *Nephrops norvegicus*. Ph.D. thesis, University of Glasgow.

PANTIN, C. F. A. (1946). *Notes on Microscopical Techniques for Zoologists*. Cambridge: Cambridge University Press.

PAUL, D. H. & MULLONEY, B. (1985*a*). Local interneurons in the swimmeret system of the crayfish. *J. comp. Physiol.* **156**, 489–502.

PAUL, D. H. & MULLONEY, B. (1985*b*). Nonspiking local interneurons in the motor pattern generator for the crayfish swimmeret. *J. Neurophysiol.* **54**, 28–43.

QUICK, D. L. J. & BRACE, R. C. (1979). Differential staining of cobalt and nickel filled neurones using rubeanic acid. *J. Microscopy* **115**, 161–163.

REICHERT, H., PLUMMER, M. R., HAGIWARA, G., ROTH, R. L. & WINE, J. J. (1982). Local interneurones in the terminal abdominal ganglion of the crayfish. *J. comp. Physiol.* **149**, 145–162.

REICHERT, H., ROWELL, C. H. F. & GRISS, C. (1985). Course correction circuitry translates feature detection into behavioural action in locusts. *Nature, Lond.* **315**, 142–144.

REICHERT, H. & WINE, J. J. (1983). Co-ordination of lateral giant and non-giant systems in crayfish escape behaviour. *J. comp. Physiol.* **153**, 3–15.

ROBERTSON, R. M. & PEARSON, K. G. (1982). A preparation for the intracellular analysis of neuronal activity during flight in the locust. *J. comp. Physiol.* **146**, 311–320.

ROWELL, C. H. F. & PEARSON, K. G. (1983). Ocellar input to the flight motor system of the locust: structure and function. *J. exp. Biol.* **103**, 265–288.

SANDEMAN, D. C. & OKAJIMA, A. (1973). Statocyst-induced eye movements in the crab, *Scylla serrata*. III. The anatomical projections of sensory and motor neurones and the response of the motor neurones. *J. exp. Biol.* **59**, 17–38.

SCHÖNE, H., NEIL, D. M., STEIN, A. & CARLSTEAD, M. K. (1976). Reactions of the spiny lobster, *Palinurus vulgaris* to substrate tilt. (I.). *J. comp. Physiol.* **107**, 113–128.

SHELTON, P. M. J., GATEN, E. & CHAPMAN, C. J. (1985). Light and retinal damage in *Nephrops norvegicus* (L.) (Crustacea). *Proc. R. Soc.* B **226**, 217–236.

TAKAHATA, M. & HISADA, M. (1982). Statocyst interneurons in the crayfish *Procambarus clarkii* Girard. I. Identification and response characteristics. *J. comp. Physiol.* **149**, 287–300.

TAKAHATA, M., NAGAYAMA, T. & HISADA, M. (1981). Physiological and morphological characterization of ananonic non-spiking interneurones in the crayfish motor control system. *Brain Res.* **226**, 309–314.

TAKAHATA, M., YOSHINO, M. & HISADA, M. (1981). The association of uropod steering with postural movement of the abdomen in crayfish. *J. exp. Biol.* **91**, 341–345.

TAKAHATA, M., YOSHINO, M. & HISADA, M. (1985). Neuronal mechanisms underlying the crayfish steering behaviour as an equilibrium response. *J. exp. Biol.* **114**, 599–617.

THEOPHILIDIS, G. & BURNS, M. D. (1982). A gold-plated suction electrode for extracellular recording and dye infusion. *J. exp. Biol.* **98**, 455–457.

WILKENS, L. A. & WOLFE, G. E. (1974). A new electrode design for *en passant* recording, stimulation and intracellular dye infusion. *Comp. Biochem. Physiol.* **48**A, 217–220.